Meiotic prophase roles of Pds5 in recombination and chromosome condensation in budding yeast[§]

Jeong Hwan Joo, Hyun Ah Kang, Keun Pil Kim[*], and Soogil Hong[*]

Department of Life Sciences, Chung-Ang University, Seoul 06974, Republic of Korea

Genetic variation in eukaryotes is mediated during meiosis by the exchange of genetic material between homologous chromosomes to produce recombinant chromosomes. Cohesin is essential to promote proper chromosome segregation, chromosome morphogenesis, and recombination in meiotic cells. Cohesin consists of three main subunits–Smc1, Smc3, and the kleisin subunit Mcd1/Scc1 (Rec8 in meiosis)–and cohesin accessory factors. In *Saccharomyces cerevisiae*, the cohesin regulatory subunit Pds5 plays a role in homolog pairing, meiotic axis formation, and interhomolog recombination. In this study, we examine the prophase functions of Pds5 by performing physical analysis of recombination and three-dimensional high-resolution microscopy analysis to identify its roles in meiosis-specific recombination and chromosome morphogenesis. To investigate whether Pds5 plays a role in mitotic-like recombination, we inhibited Mek1 kinase activity, which resulted in switching to sister template bias by Rad51-dependent recombination. Reductions in double-strand breaks and crossover products and defective interhomolog recombination occurred in the absence of Pds5. Furthermore, recombination intermediates, including single-end invasion and double-Holliday junction, were reduced in the absence of Pds5 with Mek1 kinase inactivation compared to Mek1 kinase inactivation cells. Interestingly, the absence of Pds5 resulted in increasing numbers of chromosomes with hypercompaction of the chromosome axis. Thus, we suggest that Pds5 plays an essential role in recombination by suppressing the pairing of sister chromatids and abnormal compaction of the chromosome axis.

Keywords: meiosis, recombination, Pds5, Mek1, cohesin

Introduction

Meiosis is a specialized cell division common to sexually-reproducing eukaryotes that produces four haploid daughter cells from a single diploid cell. It succeeds DNA replication, which occurs during the S-phase of the cell cycle (meiotic S-phase), and involves two successive meiotic divisions–meiosis I (MI) and meiosis II (MII). The first meiotic nuclear division (MI) separates the homologous chromosomes, leaving sister chromatids tethered together. The second equatorial division (MII) separates the sister chromatids (Zickler and Kleckner, 1999).

Meiotic recombination–the physical pairing of homologous chromosomes that occurs during the meiotic prophase before MI–is initiated by programmed double-strand breaks (DSBs) catalyzed by proteins homologous to the evolutionary conserved *Saccharomyces cerevisiae* endonuclease Spo11, a topoisomerase-like protein (Keeney, 2001; Neale *et al.*, 2005). Upon DNA cleavage, Spo11 remains covalently bound to the 5′ ends of the break, hindering resection. In budding yeast, removal of the Spo11 from meiotic DSB involves the MRX complex (Mre11/Rad50/Xrs2) and Sae2 that releases Spo11 bound to a short oligonucleotide, producing entry sites for long-range resection (Neale *et al.*, 2005).

The combined actions of 5′-3′ exonuclease Exo1, Sgs1/Top3/Rmi1 (the STR complex), and Dna2 extensively resect the short 3′ single-stranded DNA (ssDNA) tails (DSB) formed after MRX-Sae2 cleavage to generate long 3′ ssDNA (Mimitou and Symington, 2008; Zhu *et al.*, 2008; Zakharyevich *et al.*, 2010). The exposed ssDNA is immediately coated by replication protein A (RPA) to protect it from various nucleases and prevent secondary structure formation (Zakharyevich *et al.*, 2010; Garcia *et al.*, 2011; Chen and Wold, 2014). RPA is replaced by recombinase Rad51 and Dmc1 (orthologs to RecA in bacteria) and forms nucleofilaments with ssDNA in an ATP-dependent manner (Sung, 1997). The Rad51 nucleofilament then searches for a homologous template and catalyzes a strand invasion homologous DNA sequence, producing D-loop structures (San Filippo *et al.*, 2008). The invading 3′ single-strand end is extended by DNA polymerase, generating single-end invasions (SEIs) (Hunter, 2006; Oh *et al.*, 2007; Lao *et al.*, 2008; Kim *et al.*, 2010). The polymerized DNA ends are then captured as second-end DSBs by Rad52, generating double-Holliday junction (dHJs) (Hunter, 2006; Oh *et al.*, 2007; Lao *et al.*, 2008; Kim *et al.*, 2010). Finally, DNA structures are resolved and dissolved by nucleases, such as Mlh1-Mlh3/Exo1, the STR complex, Slx1-4, Mus81-Mms4, and yen1, yielding both crossover (CO) and non-crossover (NCO) products (Oh *et al.*, 2007; Jessop and Lichten, 2008; Zakharyevich *et al.*, 2010; De Muyt *et al.*, 2012; Saugar *et al.*, 2017; Wild *et al.*, 2019).

Dmc1 and meiosis-specific proteins–Hop1/Red1/Mek1–are required for inter-homolog bias during meiosis (Wan *et al.*,

2004; Niu *et al.*, 2005). A serine–threonine protein kinase, Mek1, is activated by the induction of DSBs (Niu *et al.*, 2007). During meiotic recombination, Mek1-mediated Rad54 phosphorylation suppresses complex formation between Rad51 and Rad54, and Hed1 binds to Rad51, interfering with the interaction between Rad51 and Rad54 (Niu *et al.*, 2009; Hong *et al.*, 2013; Lao *et al.*, 2013). Thus, Mek1 phosphorylation of Rad54 suppresses DSB repair via sister chromatids, so the homolog template is preferentially used over sister chromatids in the meiotic recombination pathway (Niu *et al.*, 2009; Hong *et al.*, 2013; Lao *et al.*, 2013). The meiosis-specific pathway allows homolog bias to be maintained during the transition from interhomolog-SEI to interhomolog-dHJ and promotes the formation of CO (Kim *et al.*, 2010). In the absence of Mek1 kinase activity, the meiotic DSB repair pathway switches to a mitotic-like mode via a Rad51-dependent pathway by using the sister chromatid as a template (Niu *et al.*, 2009; Kim *et al.*, 2010; Hong *et al.*, 2013; Lao *et al.*, 2013).

Cohesin is an evolutionarily conserved multi-subunit protein complex that mediates sister-chromatid cohesion (SCC) and regulates proper chromosome segregation during mitosis and meiosis (Peters *et al.*, 2008). Cohesin is also essential for chromosome axis formation during meiosis and for the regulation of meiotic S-phase progression (Hunter, 2015). In *S. cerevisiae*, the cohesin complex is a ring-shaped structure that consists of two structural maintenance chromosome subunits, Smc1 and Smc3, and a kleisin subunit, Mcd1/Scc1, in mitosis (Nasmyth and Haering, 2009; Kulemzina *et al.*, 2012; Remeseiro and Losada, 2013). During meiosis, Mcd1/Scc1 is replaced by a meiosis-specific subunit Rec8 (Klein *et al.*, 1999). Smc1 and Smc3 contain two globular hinge ATPase heads located at the N- and C-terminal domains (Haering *et al.*, 2002; Muir *et al.*, 2016). The central region of the hinge domain links the coiled-coil region via antiparallel packing (Muir *et al.*, 2016). The hinge domains of Smc1 and Smc3 form a heterodimer, and the ATPase head at the hinge domain linked with Scc1 creates a three-part ring structure that holds the sister chromatids together (Gruber *et al.*, 2003; Haering *et al.*, 2008; Muir *et al.*, 2016). Eco1-catalyzed acetylation of Smc3 is essential for cohesin establishment until the S-phase (Unal *et al.*, 2008; Zhang *et al.*, 2008). Acetylated cohesin maintains its association with chromosomes until the release of the DNA molecules (Brooker and Berkowitz, 2014). During the metaphase-to-anaphase transition, the Scc1 subunit is cleaved by cysteine protease and separase, and the cleaved cohesin is released from the sister chromatids (Rowland *et al.*, 2009; Muir *et al.*, 2016). In most eukaryotes, the cohesin complex is controlled by the cohesin accessory factors Pds5, Rad61, and Scc3 (Challa *et al.*, 2016; Muir *et al.*, 2016; Kowalec *et al.*, 2017). Pds5, the yeast homolog of Spo76, is conserved in most cells of *S. cerevisiae* (Panizza *et al.*, 2000). It is required for homolog bias establishment and maintenance, as it modulates Smc3 acetylation (Sutani *et al.*, 2009; Chan *et al.*, 2013). Pds5 is expressed and localized to the chromosome axis that mediates the establishment and maintenance of SCC and chromosome condensation in mitosis and meiosis (van Heemst *et al.*, 1999; Hartman *et al.*, 2000; Zhang *et al.*, 2005; Hong *et al.*, 2019b). During meiosis, Pds5 regulates homolog pairing and facilitates synaptonemal complex (SC) formation, axis formation, and synapsis (Jin *et al.*, 2009; Hong *et al.*, 2019b; Song *et al.*, 2021).

Previous work has suggested that in the absence of Pds5, DSB and CO formation were delayed, and the levels of DSBs and COs were lower than those in the wild-type (WT) during meiotic recombination (Hong *et al.*, 2019a). When Mek1 kinases are inactivated, homolog bias is converted to sister bias for recombination (Kim *et al.*, 2010; Hong *et al.*, 2013; Hollingsworth and Gaglione, 2019). In this study, we used physical assays to investigate whether Pds5 is involved in mitotic-like recombination caused by Mek1 inactivation. We found that inter-sister joint molecules (JMs) were reduced in the absence of Pds5 with Mek1 kinase inactivation, compared with the Mek1 kinase inactivation strain findings. We further evaluated the chromosome condensation mediated by Pds5, using 3D high resolution microscopy.

Materials and Methods

Strains

All strains were derivatives of *S. cerevisiae* SK1 strains. Detailed genotypes and strains are described in the Supplementary data Table S1. The *HIS4LEU2* locus has been described in Kim *et al.* (2010).

Meiotic time course

The experimental procedure for inducing meiosis was performed as previously described (Kim *et al.*, 2010; Hong *et al.*, 2013, 2019b; Cho *et al.*, 2016; Yoon *et al.*, 2016; Kong *et al.*, 2017). Briefly, yeast cells were spread as patches onto a YPG plate (1% yeast extract, 2% Bacto peptone, 2% Bacto agar, and 3% glycerol), and the cells were incubated at 30°C for 18 h. Selected cells from the YPG plate were streaked on a YPD plate (1% yeast extract, 2% Bacto peptone, 2% Bacto agar, and 2% glucose) for single-colony selection and incubated at 30°C for 24 h. A single colony was inoculated into 2 ml of YPD liquid medium (1% yeast extract, 2% Bacto peptone, and 2% glucose) and incubated at 30°C for 24 h to saturate the cells. To synchronize the cells to the G1 phase, the saturated cells were diluted in an SPS medium (SPS; 0.5% yeast extract, 1% Bacto peptone, 0.17% yeast nitrogen base without amino acids, 0.5% ammonium sulfate, 1% potassium acetate, and 50 mM potassium biphthalate; pH was adjusted to 5.5 with potassium hydroxide) and incubated at 30°C for 18 h. Cells synchronized at the G1 phase were harvested and resuspended in sporulation medium (SPM; 1% potassium acetate, 0.02% raffinose, and 2 drops/L antifoam) to induce meiosis. Cells were resuspended in 0.1 mg/ml trioxsalen (Sigma, T1637) and cross-linked by exposure to 365-nm UV light for 15 min. To monitor meiotic nuclear division, cells were harvested at each time point and fixed with 40% ethanol and 0.1 M sorbitol. Cells were stained with 4′,6-diamidino-2-phenylindole (DAPI) and observed using fluorescence microscopy (Olympus BX53).

Genomic DNA (gDNA) preparation

In this study, gDNA was prepared as described previously (Kim *et al.*, 2010; Hong *et al.*, 2013, 2019b; Lee *et al.*, 2015, 2021; Cho *et al.*, 2016; Yoon *et al.*, 2016; Kong *et al.*, 2017).

Briefly, cultured cells at each time point were treated with Zymolyase (US Biological, Z1004) and β-mercaptoethanol at 37°C for 30 min. Cells were lysed with guanidine-HCl solution (4.5 M guanidine-HCl, 0.1 M EDTA, 0.15 M NaCl, and 0.05% sodium lauroyl sarcosinate [sarkosyl]) at 65°C for 15 min. To remove RNA and proteins, the lysed cells were treated with RNase solution (100 mM Tris-HCl, 10 mM EDTA, and 50 mg/ml RNase [Sigma, R6513]) and proteinase K (Enzynomics, PR003). The gDNA was extracted with phenol/chloroform/isoamyl alcohol, precipitated by treatment with 3 M sodium acetate and ethanol, and the pellet dissolved in a TE buffer (50 mM Tris-HCl and 1 mM EDTA).

Physical analysis of recombination

Physical analysis of recombination in the *HIS4LUE2* locus was performed as described previously (Kim *et al.*, 2010; Hong *et al.*, 2013, 2019b; Cho *et al.*, 2016; Yoon *et al.*, 2016; Kong *et al.*, 2017; Lee *et al.*, 2021). The gDNA (2 μg) was digested with *Xho*I for one-dimensional (1D) gel analysis or with *Xho*I and *Ngo*MIV for CO/NCO gel analysis. DNA fragments were dissolved in a DNA loading buffer after precipitation with ethanol. The DNA samples were loaded onto 1D gels (0.6% UltraKem LE agarose [Young Science, Y50004] in a 1X TBE buffer), and electrophoresis was performed in a 1X TBE buffer at approximately 2 V/cM for 24 h. For two-dimensional (2D) gel analysis, gDNA (2.5 μg) was digested with *Xho*I. DNA fragments were dissolved in a DNA loading buffer after precipitation with ethanol. The DNA samples were loaded onto 1D gels (0.4% Seakem Gold agarose [Lonza, 50152] in a 1X TBE buffer), and electrophoresis was performed in a 1X TBE buffer at approximately 1 V/cM for 21 h. For the second-dimension of electrophoresis, the 1D gel was stained with 0.5 μg/ml ethidium bromide (EtBr), the gel strips of interest were placed in 2D gels (0.8% UltraKem LE agarose containing EtBr in 1X TBE buffer), and electrophoresis was performed in a 1X TBE buffer at 6 V/cM for 6 h in a cold room. DNA was transferred to a Nylon membrane to prepare for southern blot analysis. Hybridization was carried out using labeled ^{32}P-dCTP radioactive nucleotides reacted with a random primer labeling mixture (Agilent Technologies, 300392). Hybridization signals were observed using a phospho-image analyzer (Bio-Rad). Hybridized DNA signals, such as DSBs, SEIs, dHJs, and COs, were quantified using Quantity One software (Bio-Rad).

Chromosome spreading and immunofluorescence

Chromosome spreads for immunofluorescence analysis were prepared as described previously (Yoon *et al.*, 2016; Hong *et al.*, 2019b). Briefly, cells were lysed and fixed onto clean slides using 1% Lipsol and 3% paraformaldehyde containing 3.4% sucrose. Then, the slides were soaked in 0.2% Photo-Flo (Kodak, 146-4510), transferred to a TBS buffer (136 mM NaCl, 3 mM KCl, and 25 mM Tris-HCl; pH 8.0), and incubated for 15 min. For immunostaining, the following antibodies were used: rabbit polyclonal Zip1 antibody (diluted 1:200; Santa Cruz Biotechnology, sc-33733); primary mouse monoclonal Myc antibody (diluted 1:200; Santa Cruz Biotechnology, sc-40); secondary TRITC-conjugated goat anti-rabbit lgG (diluted 1:300; Jackson ImmunoResearch, 111-025-003); and secon-

dary Alexa 488-conjugated goat anti-mouse IgG (diluted 1:300; Jackson ImmunoResearch, 115-545-003). Images were acquired using a Nikon Eclipse Ti fluorescence microscope equipped with a Nikon DS-Qi2 monochrome camera. Super-resolution images were obtained by structured illumination microscopy (SIM) using a Nikon Eclipse Ti-E equipped with an EM CCD camera iXon897 and 100× oil objective (NA 1.49). Image stacks were reconstructed using Nikon NIS software. Deconvolution was adjusted with Nikon NIS software.

Results

Pds5 and Mek1 are involved in DSB and CO formation

We investigated the progression of Rad51-dependent homologous recombination in the *mek1as* and *mek1as pCLB2-PDS5* strains. *Mek1as* encodes mutant Mek1 proteins whose activities are blocked by the chemical inhibitor 1-NA-PP1 (IN) during meiosis (Niu *et al.*, 2005; Kim *et al.*, 2010; Hong *et al.*, 2013, 2019b). It is also known that *pCLB2* is suppressed during meiosis (Lee and Amon, 2003). We monitored the progression of meiotic recombination at the *HIS4LEU2* hotspot integrated into chromosome III by using standard physical assays of DNA (Kim *et al.*, 2010; Hong *et al.*, 2013, 2019b). The standard physical assays combined with 1D gel analysis separated DNA fragments by size, and 2D gel analysis separated DNA fragments by size and shape. Southern blotting allowed for visualization of the key meiotic recombination steps to hybridize the appropriate probe (probe A) (Kim *et al.*, 2010; Hong *et al.*, 2013, 2019b). DSBs and COs can be analyzed using 1D gel analysis. In addition, the kinetics of inter-homolog-crossovers (IH-COs) and inter-homolog-non-crossovers (IH-NCOs) can be revealed by 1D gel analysis using *Xho*I and *Ngo*MIV restriction polymorphisms (Fig. 1A and B; Hunter and Kleckner, 2001; Oh *et al.*, 2007; Kim *et al.*, 2010; Hong *et al.*, 2019b). Thus, we monitored the progression of DSBs and COs through 1D gel analysis. In *mek1as*(-IN)–the *mek1as* strain untreated with the 1-NA-PP1 inhibitor–DSBs appeared at 2.5 h, peaked at 4 h, and disappeared in a timely fashion. In addition, COs appeared at 3.5 h and reached a high level of 18.48% at a later time point. In *mek1as*(+IN)–the *mek1as* strain treated with the 1-NA-PP1 inhibitor–DSBs exhibited hyper-resection and reached 1.41% at 3.5 h. In addition, the maximum level of COs was 1.11% at 24 h (Fig. 1C and D).

In *mek1as*(-IN) *pCLB2-PDS5*, few DSBs appeared at 2.5 h, then peaked at 2.98% at 5 h, followed by a slow decrease. CO formation appeared at 6 h and reached a maximum level of 6.41% at 24 h (Fig. 1C and D). In *mek1as*(+IN) *pCLB2-PDS5*, very few DSBs could be found at 2.5 h, which peaked at 5 h, then disappeared gradually. COs were generated at 5 h and peaked at 0.87% (Fig. 1C and D). When the Mek1 function was abolished, the *PDS5* gene was required to ensure proper formation and processing of DSB and CO formation, but the levels were slightly lower than those in *mek1as*(+IN).

Next, we investigated the progression of IH-COs and IH-NCOs (Fig. 1E and F). The gDNA was digested with *Xho*I and *Ngo*MVI, followed by 1D gel analysis (Fig. 1A, B, and E). In *mek1as*(-IN), IH-COs and IH-NCOs appeared later and persisted longer. IH-CO and IH-NCO levels were both increased
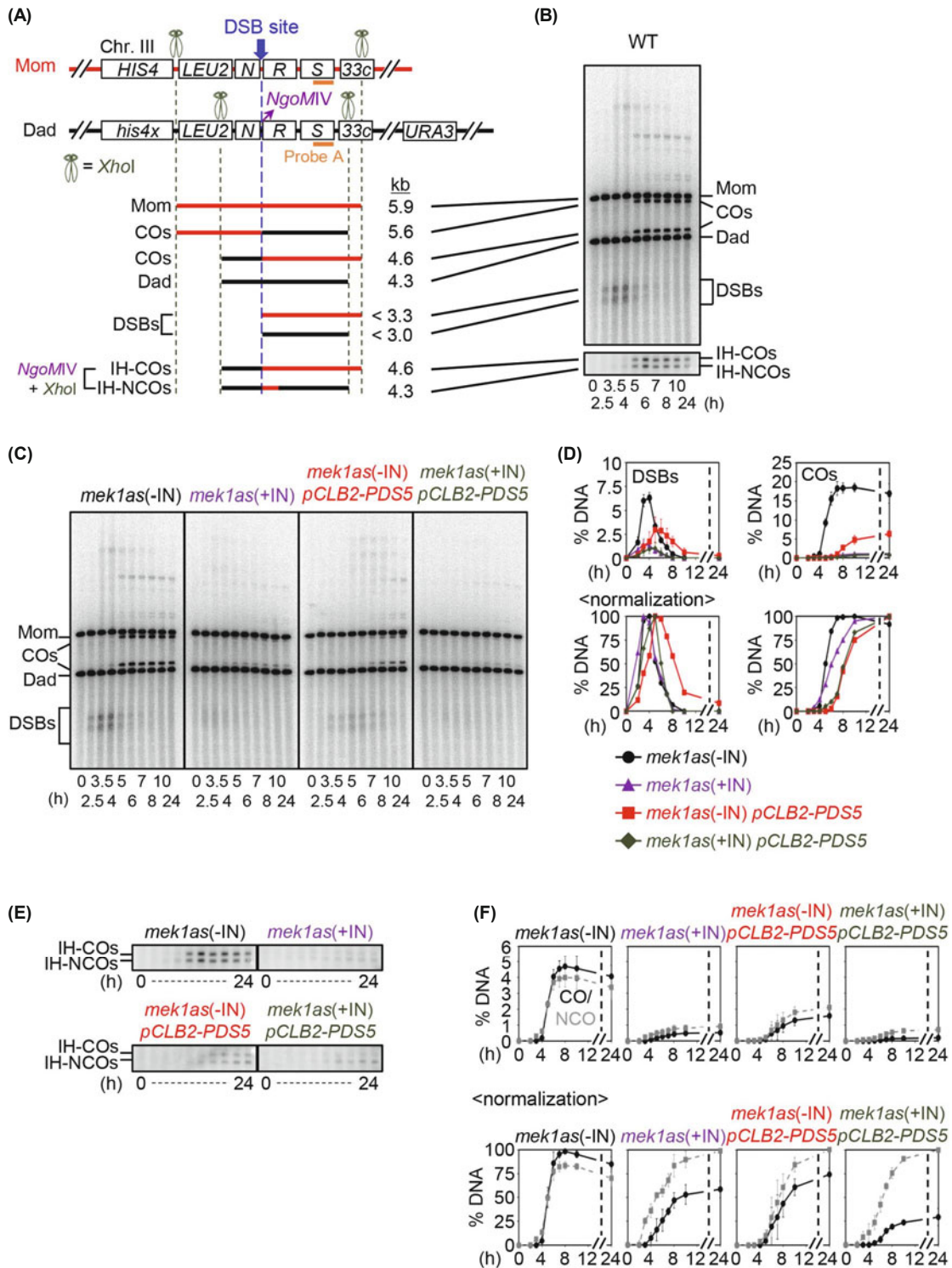
Fig. 1. **The physical map and CO formation in *mek1as* and *pCLB2-PDS5 mek1as* strains.** (A) Physical map of the *HIS4LEU2* hotspot located on chromosome III showing diagnostic restriction sites and the position of probe A (Kim *et al.*, 2010). Mom and dad species were distinguished with *XhoI* restriction polymorphisms. DNA fragments were separated by 1D gels and detected by Southern blot hybridization with probe A (Kim *et al.*, 2010). N, *NFS1*; R, *RRP7*; S, *STE50*. DSBs, double-strand breaks; COs, crossovers; IH-CO, interhomolog-crossover; IH-NCO, interhomolog-noncrossover. (B) Representative images of 1D gel analysis showing DSBs and COs. (C) 1D gel analysis of DSBs and COs in *mek1as* and *mek1as pCLB2-PDS5* strains in the presence or absence of 1-NA-PP1. Meiosis was induced in SPM medium. 1-NA-PP1 was treated at 0 h. -IN, untreated 1-NA-PP1; +IN, treated 1-NA-PP1. (D) Top, Quantification of DSBs and COs shown in (C). Bottom, DSB and CO levels over time are plotted as the maximum percentage of the most abundant species. The data indicate the mean ± SD (n = 3). (E) Representative images of 1D gel analysis showing IH-COs and IH-NCOs in *mek1as* and *mek1as pCLB2-PDS5* strains in the presence or absence of 1-NA-PP1. (F) Top, quantification of IH-COs and IH-NCOs shown in (E); Bottom, IH-CO and IH-NCO levels over time are plotted as the maximum percentage of the most abundant IH-CO or IH-NCO levels. The data indicate the mean ± SD (n = 3).
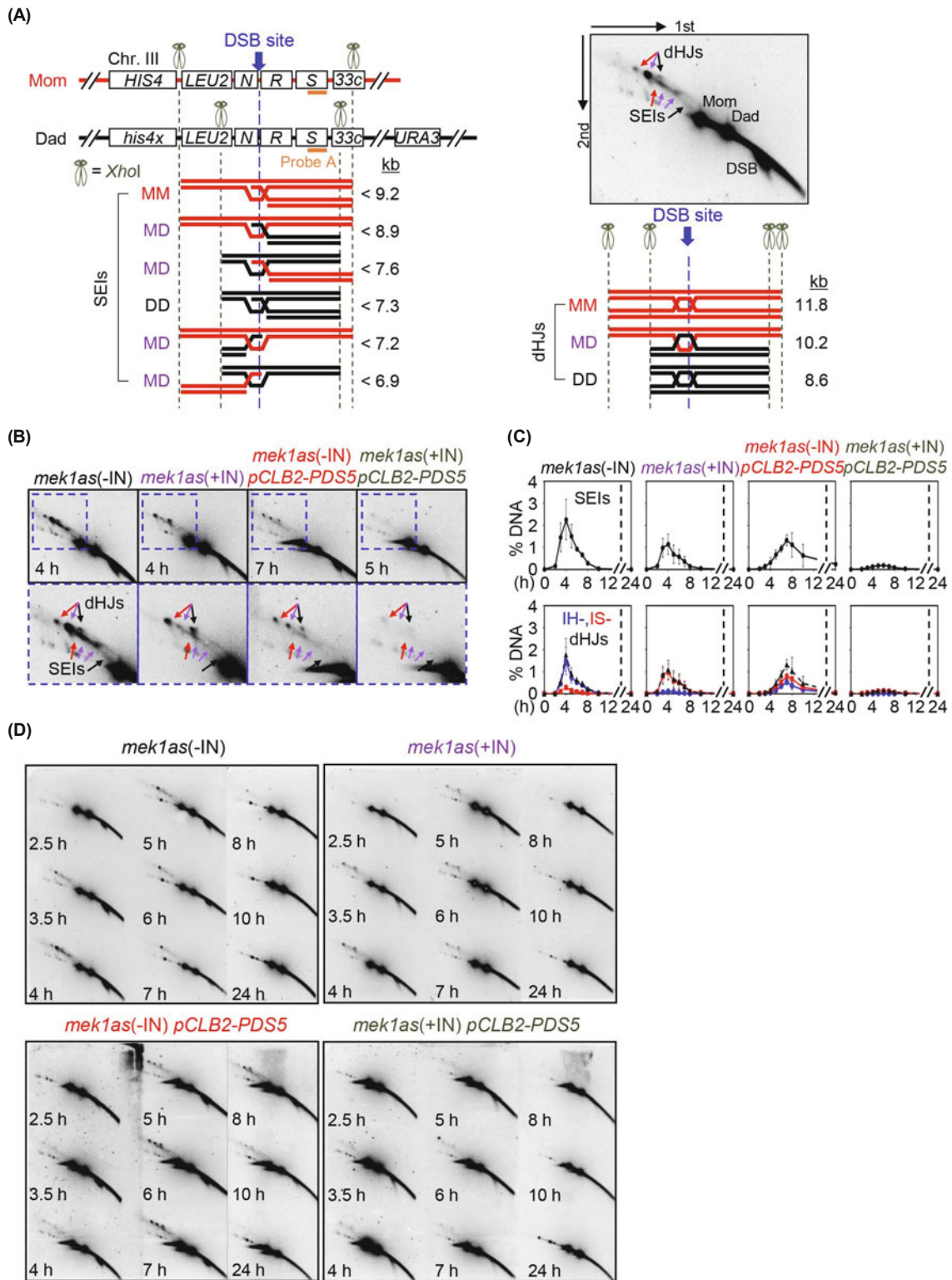
Fig. 2. Joint molecule formation of *mek1as* and *mek1as pCLB2-PDS5* strains in the presence or absence of inhibitor. (A) 2D gel analysis of JM species. Physical map showing the diagnostic restriction sites and the position of probe A (Kim *et al.*, 2010). DNA fragments were separated by 2D gels and detected by southern blot hybridization with probe A. MM, inter-sister Mom-Mom; MD, interhomolog Mom-Dad; DD, inter-sister Dad–Dad; SEIs, single-end invasions; dHJs, double-Holliday junctions. Representative images of 2D gel analysis showing dHJs and SEIs. (B) 2D gel analysis of SEIs and dHJs in the *mek1as* and *mek1as pCLB2-PDS5* strains in the presence or absence of 1-NA-PP1. The blue dashed square shows the JM region. IH-, IS-SEI and IH-, IS-dHJ species are indicated with arrows. Red arrows, Mom–Mom IS-JMs; black arrows, Dad–Dad IS-JMs; purple arrows, Mom–Dad IH-JMs. (C) Quantification of SEIs and dHJs shown in (D). The data indicate the mean ± SD (n = 3). (D) Whole images of 2D gel in *mek1as* and *mek1as pCLB2-PDS5* strains in the presence or absence of 1-NA-PP1.
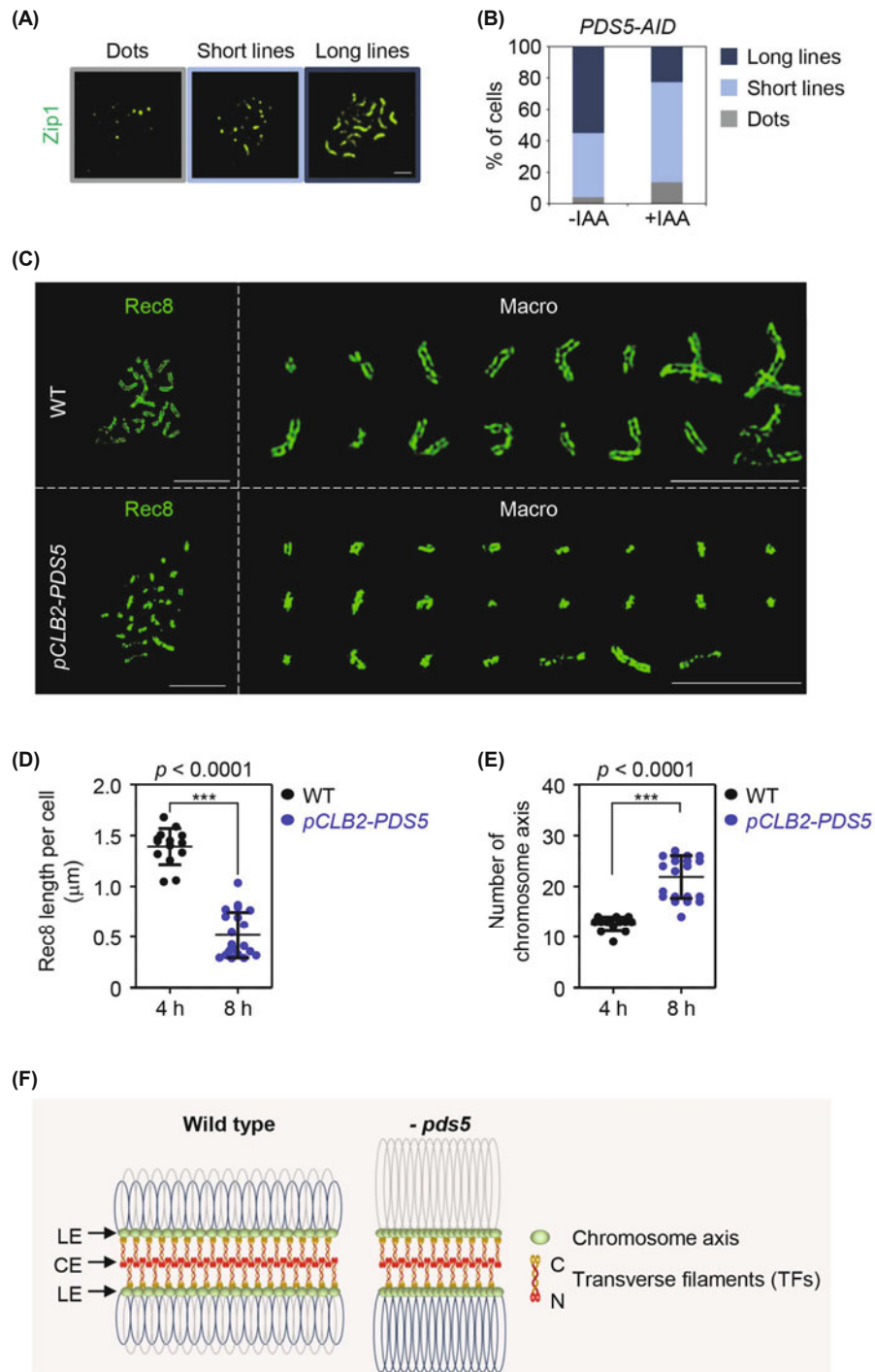
Fig. 3. Analysis of synaptonemal complex formation in the presence or absence of Pds5. (A) The chromosome spreads of meiotic cells were immunostained with Zip1. Zip1 staining was categorized into three classes: dots, dotted Zip1 staining; short lines, discontinuous Zip1 staining; long lines, full Zip1 staining. The scale bars indicate 2.5 µm. (B) Analysis of Zip1 assembly in *PDS5-AID* staining. Meiosis was induced in SPM medium in the presence or absence of auxin. Auxin (2 mM) treatment was performed at 0.5 h to induce degradation of Pds5. -IAA, untreated auxin; +IAA, treated auxin; dark blue, long lines; blue, short lines; gray, dots. (C) Left, SIM images at the pachytene chromosome in the WT and *pCLB2-PDS5* strains. The chromosome spreads of meiotic cells were immunostained with anti-HA (For Rec8-3HA). The scale bar represents 2.5 µm. Right, Individually cropped chromosome axis in WT and *pCLB2-PDS5* strains. The scale bar represents 2.5 µm. (D) Comparison of axis length per cell between the WT and *pCLB2-PDS5* mutant. Error bars indicate mean ± SD. *P*-values were determined by Student's *t*-test. (E) Number of chromosome axes in the WT and *pCLB2-PDS5* mutant. Error bars indicate mean ± SD. *P*-values were determined by Student's *t*-test. (F) Schematic explanation of synaptonemal complex (SC) formation and chromosome compaction at pachytene stage. SC is composed of two lateral elements (LEs) and a central element (CE). LEs are composed of meiosis-specific Hop1, Red1, and cohesin complexes that contain the meiosis-specific kleisin subunit, Rec8. In the CE, transverse filaments (TFs) protein, Zip1, are assembled between homologous chromosomes. In the absence of Pds5, meiotic chromosomes show hypercompaction, and homologs fail to pair, resulting in inter-sister SC formation. C, C-terminus of Zip1 protein; N, N-terminus of Zip1 protein.

in *mek1as*(-IN) compared to levels in *mek1as*(+IN) (4.70% and 4.00% vs. 0.52% and 0.91%, respectively) and were reduced by approximately 1.5 fold in *mek1as*(-IN) *pCLB2-PDS5* (1.58% and 2.11%, respectively; Fig. 1E and F). The lowest levels of IH-CO and IH-NCO were detected in *mek1as*(+IN) *pCLB2-PDS5* at 0.21% and 0.70%, respectively, and showed similar delays in formation to *mek1as*(+IN) (Fig. 1E and F). Altogether, these results indicate that Pds5 is essential for DSB and CO formation, including IH-COs and IH-NCOs, regardless of whether Mek1 is present.

Pds5 is involved in Mek1-dependent JM formation

The progression of meiotic recombination at the *HIS4LEU2* hotspot was monitored by 2D gel electrophoresis, which identifies SEIs and dHJs, two well-known sequential CO-designated JMs (Fig. 2A; Hunter and Kleckner, 2001; Oh *et al.*, 2007). This analysis can also distinguish inter-homolog and inter-sister JMs (the ratio of IH-dHJs:IS-dHJs) by characterizing differences in size and shape (Fig. 2A; Kim *et al.*, 2010; Hong *et al.*, 2013, 2019b).

We analyzed SEI and dHJ formation in the *mek1as* and *mek1as pCLB2-PDS5* strains in the presence or absence of Mek1 kinase activity (Fig. 2C). Peak SEI levels were higher in *mek1as*(-IN) than *mek1as*(+IN), at 2.25% and 1.15%, respectively, at 4 h. In *mek1as*(-IN) *pCLB2-PDS5*, the peak SEI level was 1.32% at 7 h. In the absence of Mek1 kinase activity, the peak SEI level for *mek1as*(+IN) *pCLB2-PDS5* was 0.19% at 6 h. IH-dHJ and IS-dHJ levels were 1.48% and 0.29% (IH-dHJs:IS-dHJs = 5.18:1), respectively, in *mek1as*(-IN). In *mek1as*(+IN), IH-dHJs decreased to almost 0.12%, but IS-dHJs showed a compensatory increase to 0.97% (IH-dHJs:IS-dHJs = 1:8.34). These results show that when Mek1 kinases are inactivated under the meiotic recombination pathway, the homolog bias is converted from inter-homolog to inter-sister to repair recombination. This phenomenon is similar to our previous studies (Kim *et al.*, 2010; Hong *et al.*, 2013; Cho *et al.*, 2016). In *mek1as*(-IN) *pCLB2-PDS5*, the maximum level of IH-dHJs was 0.53% and that of IS-dHJs was 0.79% at 7 h (IH-dHJs:IS-dHJs = 1:1.48) (Fig. 2C). Previous studies have shown that equivalent levels of IH-dHJs and IS-dHJs are generated in the absence of homolog-bias maintenance in the *pCLB2-PDS5* and *rec8Δ* strains (Kim *et al.*, 2010; Hong *et al.*, 2019b). In *mek1as*(+IN) *pCLB2-PDS5*, the maximum level of IH-dHJs was 0.02% and that of IS-dHJs was 0.13%

at 6 h (IH-dHJs:IS-dHJs = 1:8.31) (Fig. 2C). The level of IS-dHJs in the *mek1as*(+IN) *pCLB2-PDS5* strain showed a greater decrease than in the *mek1as*(+IN) strain. This result indicates that Pds5 is required for DSB repair via the sister chromatid in the absence of Mek1 kinase activity.

Pds5 is required for homolog pairing and SC formation in meiotic recombination

During meiotic recombination, the synaptonemal complex (SC) forms two parallel lines between homologous chromosomes (Jin *et al.*, 2009). The meiosis-specific *pds5* null mutant, *pCLB2-PDS5*, shows defects in homolog pairing and SC formation (Jin *et al.*, 2009; Hong *et al.*, 2019b). Thus, the absence of Pds5 yields a shorter SC than in the WT and forms an SC between sister chromatids (Fig. 3F; Jin *et al.*, 2009; Hong *et al.*, 2019b). In *S. cerevisiae*, Zip1 is one of the SC components required for meiotic chromosome synapsis between homologs (Sym *et al.*, 1993; Hong *et al.*, 2019b). In the absence of Pds5, chromosomes do not progress to full-length chromosomes, indicating a defect in the chromosome transition from zygotene to pachytene (Hong *et al.*, 2019b). We used the auxin-inducible degron system to deplete Pds5, which is rapidly degraded after treatment with auxin (Morawska and Ulrich, 2013; Hong *et al.*, 2019b). We stained chromosomes and proteins using anti-Zip1 and DAPI on chromosome spreads and observed the Zip1 protein. Zip1 assembly was categorized into dot chromosomes (dots), short or discontinuous chromosomes (short lines), and full-length chromosomes (long lines) (Fig. 3A). In the *PDS5-AID* strain not treated with auxin (*PDS5-AID*-IAA), full-length chromosomes constituted approximately 42% of the chromosomes. However, in the *PDS5-AID* strain treated with auxin (*PDS5-AID* +IAA), full-length chromosomes were reduced by approximately 24%, and short-length chromosomes were increased by approximately 65% (Fig. 3B). These data suggest that the absence of Pds5 causes defects in SC formation in meiotic recombination.

Alterations in Pds5 protein levels directly alter chromosome axis length; however, Rec8 primarily regulates the axis indirectly by regulating Pds5 abundance, so we observed the meiotic chromosome axis using high-resolution SIM (Fig. 3C). In the WT, Rec8 localized in parallel lines, which corresponded to two full-length axes. Although *pCLB2-PDS5* also exhibited parallel axis lines, the axis length was comparatively shorter (the average length of the axis was 1.39 ±
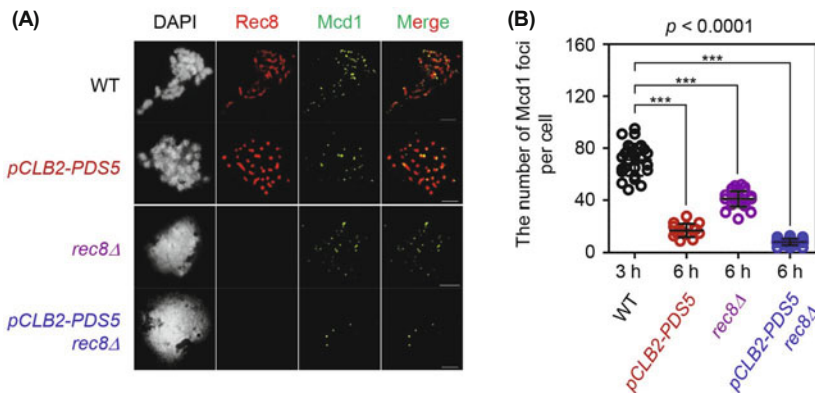
Fig. 4. Focus number of Mcd1 in WT, *pCLB2-PDS5*, *rec8Δ*, and *pCLB2-PDS5 rec8Δ*. (A) The chromosome spreads of meiotic cells were immunostained with anti-HA (for Rec8-3HA) and anti-Myc (for Mcd1-9Myc) in WT, *pCLB2-PDS5*, *rec8Δ*, and *pCLB2-PDS5 rec8Δ*. The scale bar represents 2.5 μm. (B) Number of Mcd1 foci in the WT (at 3 h), *pCLB2-PDS5* (at 6 h), *rec8Δ* (at 6 h), and *pCLB2-PDS5 rec8Δ* (at 6 h). Error bars indicate mean ± SD. *P*-values for all relevant comparisons are determined by Student's *t*-test.

0.17 μm *vs.* 0.51 ± 0.22 μm; Fig. 3C and D). Therefore, the axis length is shorter when Pds5 is absent. We also quantified the Rec8 lines per cell. There were fewer Rec8 lines per cell in the WT than in the *pCLB2-PDS5* mutant (12.57 ± 1.34 *vs.* 21.85 ± 4.09; Fig. 3E). In addition, we counted the number of Ctf19 foci, which is one of the centromere components (Supplementary data Fig. S1A; Tsubouchi *et al.*, 2008). In the *ndt80Δ* strain, which is a meiosis-specific transcription factor required for exit from pachytene, the number of Ctf19 foci colocalized with the Zip1 chromosome was approximately 14 ± 2 at 8 h (Supplementary data Fig. S1B). In the *ndt80Δ pCLB2-PDS5* strain, *pds5* meiotic-null mutants had 21 ± 3.7 Ctf19 foci per cell (Supplementary data Fig. S1B). Similar to the Zip1 abundance, the number of Ctf19 foci increased in the absence of Pds5. These data demonstrate that when Pds5 is absent, the number of Rec8 lines is doubled compared to the WT. Thus, Pds5 inhibits the hypercompaction of chromosome axes and pairing between homologous chromosomes (Fig. 3F).

Pds5 and Rec8 are required for Mcd1 localization

According to Hong *et al.* (2019b), Pds5 affects Mcd1 localization, and Rec8 and Mcd1 are localized to different regions on the chromosomes during meiosis. Therefore, we quantified the number of Mcd1 foci in the absence of Pds5 and Rec8 (Fig. 4A). The number of Mcd1 foci in the WT was 61.1 ± 10.16 at 4 h, which decreased dramatically in the absence of Pds5 to 15.6 ± 4.69 at 8 h, but less so in the absence of Rec8 to 31.57 ± 6.12 at 8 h (Fig. 4B). In the *pCLB2-PDS5 rec8Δ* strains, the number of Mcd1 foci was absolutely diminished (4.43 ± 2.33; Fig. 4B).

Discussion

In most eukaryotes, including budding yeast, plant, and mammals, cohesin plays a key role in genetic recombination during meiosis (Brooker and Berkowitz, 2014). Cohesin also functions in DSB formation, homolog-bias maintenance, and homolog synapsis (Kim *et al.*, 2010; Brooker and Berkowitz, 2014; Hong *et al.*, 2019a). Pds5 contributes to homolog pairing, axis formation, and recombination as one of the regulatory factors of cohesin (Jin *et al.*, 2009; Hong *et al.*, 2019b). The absence of Pds5 increases the number of inter-sister JMs due to a defect in synapsis formation between homologs (Jin *et al.*, 2009; Hong *et al.*, 2019b), but this process is independent of Rec8 functions (Hong *et al.*, 2019b). Furthermore, Pds5 plays a role in the maintenance of homolog-bias independent of Rec8. Mek1 kinase inactivation prevents homolog bias, and thus the recombination pathway is converted from homolog template bias to sister template bias. In addition, the ssDNA ends flanking a DSB are required to search for sister chromatids, which are preferred partner templates for DSB repair in mitotic diploid yeast cells (Niu *et al.*, 2009; Hong *et al.*, 2013; Lao *et al.*, 2013).

We investigated whether Pds5 is involved in Rad51-dependent recombination (Mek1 inactivation condition) in meiotic recombination. Interestingly, the absence of Pds5 without Mek1 kinase activity, *mek1as*(+IN), showed a low level of IS-dHJs compared to *mek1as*(-IN), implying that Pds5 is required for sister recombination in the Mek1-dependent pathway.

During meiosis, SCs form two parallel lines between homologous chromosomes to promote their pairing and mediate CO recombination (Schmekel and Daneholt, 1995; Jin *et al.*, 2009; Hollingsworth, 2020). Pds5 localizes on the chromosome axis and regulates homolog pairing and synapsis (Jin *et al.*, 2009; Hong *et al.*, 2019b). The absence of Pds5 manifests as chromosome condensation, resulting in hypercompaction of the chromosome axis (Ding *et al.*, 2006; Jin *et al.*, 2009; Hong *et al.*, 2019b). Furthermore, the absence of Pds5 confers failure of homolog pairing, resulting in an increased number of chromosomes. Interestingly, in the absence of Pds5, the formation of short parallel lines between chromosomes was observed with super-resolution microscopy, implying that Pds5 is involved in the modulation of chromosome axis formation and promotes proper chromosome morphogenesis during meiosis. Thus, Pds5 may modulate chromosome axis formation and proper chromosome condensation process.

Mcd1 can be functional even in the presence of the meiotic kleisin subunit Rec8 in meiosis (Hong *et al.*, 2019b). Thus, Pds5 might be associated with Mcd1 to modulate stabilization of the cohesin complex (D'Ambrosio and Lavoie, 2014). Moreover, in the absence of Pds5, the number of Mcd1 foci is dramatically reduced, implying that Pds5 supports the stabilization of Mcd1 in meiosis. This result suggests that Pds5 might modulate the localization of Mcd1 during meiosis via a meiosis-specific pathway.

Acknowledgements

Conflict of Interest

The authors have no conflict of interest to report.

References

Brooker, A.S. and Berkowitz, K.M. 2014. The roles of cohesins in mitosis, meiosis, and human health and disease. *Methods Mol. Biol.* **1170**, 229–266.

Challa, K., Lee, M.S., Shinohara, M., Kim, K.P., and Shinohara, A. 2016. Rad61/Wpl1 (Wapl), a cohesin regulator, controls chromosome compaction during meiosis. *Nucleic Acids Res.* **44**, 3190–3203.

Chan, K.L., Gligoris, T., Upcher, W., Kato, Y., Shirahige, K., Nasmyth, K., and Beckouët, F. 2013. Pds5 promotes and protects cohesin acetylation. *Proc. Natl. Acad. Sci. USA* **110**, 13020–13025.

Chen, R. and Wold, M.S. 2014. Replication protein A: single-stranded DNA's first responder. *BioEssays* **36**, 1156–1161.

Cho, H.R., Kong, Y.J., Hong, S.G., and Kim, K.P. 2016. Hop2 and Sae3 are required for Dmc1-mediated double-strand break repair via homolog bias during meiosis. *Mol. Cells* **39**, 550–556.

D'Ambrosio, L.M. and Lavoie, B.D. 2014. Pds5 prevents the Poly-

SUMO-dependent separation of sister chromatids. *Curr. Biol.* **24**, 361–371.

De Muyt, A., Jessop, L., Kolar, E., Sourirajan, A., Chen, J., Dayani, Y., and Lichten, M. 2012. BLM helicase ortholog Sgs1 is a central regulator of meiotic recombination intermediate metabolism. *Mol. Cell* **46**, 43–53.

Ding, D.Q., Sakurai, N., Katou, Y., Itoh, T., Shirahige, K., Haraguchi, T., and Hiraoka, Y. 2006. Meiotic cohesins modulate chromosome compaction during meiotic prophase in fission yeast. *J. Cell Biol.* **174**, 499–508.

Garcia, V., Phelps, S.E., Gray, S., and Neale, M.J. 2011. Bidirectional resection of DNA double-strand breaks by Mre11 and Exo1. *Nature* **479**, 241–244.

Gruber, S., Haering, C.H., and Nasmyth, K. 2003. Chromosomal cohesin forms a ring. *Cell* **112**, 765–777.

Haering, C.H., Farcas, A.M., Arumugam, P., Metson, J., and Nasmyth, K. 2008. The cohesin ring concatenates sister DNA molecules. *Nature* **454**, 297–301.

Haering, C.H., Löwe, J., Hochwagen, A., and Nasmyth, K. 2002. Molecular architecture of SMC proteins and the yeast cohesin complex. *Mol. Cell* **9**, 773–788.

Hartman, T., Stead, K., Koshland, D., and Guacci, V. 2000. Pds5p is an essential chromosomal protein required for both sister chromatid cohesion and condensation in *Saccharomyces cerevisiae*. *J. Cell Biol.* **151**, 613–626.

Hollingsworth, N.M. 2020. A new role for the synaptonemal complex in the regulation of meiotic recombination. *Genes Dev.* **34**, 1562–1564.

Hollingsworth, N.M. and Gaglione, R. 2019. The meiotic-specific Mek1 kinase in budding yeast regulates interhomolog recombination and coordinates meiotic progression with double-strand break repair. *Curr. Genet.* **65**, 631–641.

Hong, S., Joo, J.H., Yun, H., and Kim, K.P. 2019a. The nature of meiotic chromosome dynamics and recombination in budding yeast. *J. Microbiol.* **57**, 221–231.

Hong, S., Joo, J.H., Yun, H., Kleckner, N., and Kim, K.P. 2019b. Recruitment of Rec8, Pds5 and Rad61/Wapl to meiotic homolog pairing, recombination, axis formation and S-phase. *Nucleic Acids Res.* **47**, 11691–11708.

Hong, S., Sung, Y., Yu, M., Lee, M., Kleckner, N., and Kim, K.P. 2013. The logic and mechanism of homologous recombination partner choice. *Mol. Cell* **51**, 440–453.

Hunter, N. 2006. Meiotic recombination. *In* Aguilera, A. and Rothstein, R. (eds.), Molecular Genetics of Recombination, pp. 381–442. Springer, Berlin, Heidelberg, Germany.

Hunter, N. 2015. Meiotic recombination: the essence of heredity. *Cold Spring Harb. Perspect. Biol.* **7**, a016618.

Hunter, N. and Kleckner, N. 2001. The single-end invasion: an asymmetric intermediate at the double-strand break to double-Holliday junction transition of meiotic recombination. *Cell* **106**, 59–70.

Jessop, L. and Lichten, M. 2008. Mus81/Mms4 endonuclease and Sgs1 helicase collaborate to ensure proper recombination intermediate metabolism during meiosis. *Mol. Cell* **31**, 313–323.

Jin, H., Guacci, V., and Yu, H.G. 2009. Pds5 is required for homologue pairing and inhibits synapsis of sister chromatids during yeast meiosis. *J. Cell Biol.* **186**, 713–725.

Keeney, S. 2001. Mechanism and control of meiotic recombination initiation. *Curr. Top. Dev. Biol.* **52**, 1–53.

Kim, K.P., Weiner, B.M., Zhang, L., Jordan, A., Dekker, J., and Kleckner, N. 2010. Sister cohesion and structural axis components mediate homolog bias of meiotic recombination. *Cell* **143**, 924–937.

Klein, F., Mahr, P., Galova, M., Buonomo, S.B., Michaelis, C., Nairz, K., and Nasmyth, K. 1999. A central role for cohesins in sister chromatid cohesion, formation of axial elements, and recombination during yeast meiosis. *Cell* **98**, 91–103.

Kong, Y.J., Joo, J.H., Kim, K.P., and Hong, S. 2017. Hed1 promotes meiotic crossover formation in *Saccharomyces cerevisiae*. *J. Micro-*

biol. Biotechnol. **27**, 405–411.

Kowalec, P., Fronk, J., and Kurlandzka, A. 2017. The Irr1/Scc3 protein implicated in chromosome segregation in *Saccharomyces cerevisiae* has a dual nuclear-cytoplasmic localization. *Cell Div.* **12**, 1.

Kulemzina, I., Schumacher, M.R., Verma, V., Reiter, J., Metzler, J., Failla, A.V., Lanz, C., Sreedharan, V.T., Rätsch, G., and Ivanov, D. 2012. Cohesin rings devoid of Scc3 and Pds5 maintain their stable association with the DNA. *PLoS Genet.* **8**, e1002856.

Lao, J.P., Cloud, V., Huang, C.C., Grubb, J., Thacker, D., Lee, C.Y., Dresser, M.E., Hunter, N., and Bishop, D.K. 2013. Meiotic crossover control by concerted action of Rad51-Dmc1 in homolog template bias and robust homeostatic regulation. *PLoS Genet.* **9**, e1003978.

Lao, J.P., Oh, S.D., Shinohara, M., Shinohara, A., and Hunter, N. 2008. Rad52 promotes postinvasion steps of meiotic double-strand-break repair. *Mol. Cell* **29**, 517–524.

Lee, B.H. and Amon, A. 2003. Role of polo-like kinase CDC5 in programming meiosis I chromosome segregation. *Science* **300**, 482–486.

Lee, M.S., Higashide, M.T., Choi, H., Li, K., Hong, S., Lee, K., Shinohara, A., Shinohara, M., and Kim, K.P. 2021. The synaptonemal complex central region modulates crossover pathways and feedback control of meiotic double-strand break formation. *Nucleic Acids Res.* **49**, 7537–7553.

Lee, M.S., Yoon, S.W., and Kim, K.P. 2015. Mitotic cohesin subunit Mcd1 regulates the progression of meiotic recombination in budding yeast. *J. Microbiol. Biotechnol.* **25**, 598–605.

Mimitou, E.P. and Symington, L.S. 2008. Sae2, Exo1 and Sgs1 collaborate in DNA double-strand break processing. *Nature* **455**, 770–774.

Morawska, M. and Ulrich, H.D. 2013. An expanded tool kit for the auxin-inducible degron system in budding yeast. *Yeast* **30**, 341–351.

Muir, K.W., Kschonsak, M., Li, Y., Metz, J., Haering, C.H., and Panne, D. 2016. Structure of the Pds5-Scc1 complex and implications for cohesin function. *Cell Rep.* **14**, 2116–2126.

Nasmyth, K. and Haering, C.H. 2009. Cohesin: its roles and mechanisms. *Annu. Rev. Genet.* **43**, 525–558.

Neale, M.J., Pan, J., and Keeney, S. 2005. Endonucleolytic processing of covalent protein-linked DNA double-strand breaks. *Nature* **436**, 1053–1057.

Niu, H., Li, X., Job, E., Park, C., Moazed, D., Gygi, S.P., and Hollingsworth, N.M. 2007. Mek1 kinase is regulated to suppress double-strand break repair between sister chromatids during budding yeast meiosis. *Mol. Cell. Biol.* **27**, 5456–5467.

Niu, H., Wan, L., Baumgartner, B., Schaefer, D., Loidl, J., and Hollingsworth, N.M. 2005. Partner choice during meiosis is regulated by Hop1-promoted dimerization of Mek1. *Mol. Biol. Cell* **16**, 5804–5818.

Niu, H., Wan, L., Busygina, V., Kwon, Y., Allen, J.A., Li, X., Kunz, R.C., Kubota, K., Wang, B., Sung, P., *et al.* 2009. Regulation of meiotic recombination via Mek1-mediated Rad54 phosphorylation. *Mol. Cell* **36**, 393–404.

Oh, S.D., Lao, J.P., Hwang, P.Y., Taylor, A.F., Smith, G.R., and Hunter, N. 2007. BLM ortholog, Sgs1, prevents aberrant crossing-over by suppressing formation of multichromatid joint molecules. *Cell* **130**, 259–272.

Panizza, S., Tanaka, T., Hochwagen, A., Eisenhaber, F., and Nasmyth, K. 2000. Pds5 cooperates with cohesin in maintaining sister chromatid cohesion. *Curr. Biol.* **10**, 1557–1564.

Peters, J.M., Tedeschi, A., and Schmitz, J. 2008. The cohesin complex and its roles in chromosome biology. *Genes Dev.* **22**, 3089–3114.

Remeseiro, S. and Losada, A. 2013. Cohesin, a chromatin engagement ring. *Curr. Opin. Cell Biol.* **25**, 63–71.

Rowland, B.D., Roig, M.B., Nishino, T., Kurze, A., Uluocak, P., Mishra, A., Beckouët, F., Underwood, P., Metson, J., Imre, R., *et al.* 2009. Building sister chromatid cohesion: Smc3 acetylation

counteracts an antiestablishment activity. *Mol. Cell* **33**, 763–774.

San Filippo, J., Sung, P., and Klein, H. 2008. Mechanism of eukaryotic homologous recombination. *Annu. Rev. Biochem.* **77**, 229–257.

Saugar, I., Jiménez-Martín, A., and Tercero, J.A. 2017. Subnuclear relocalization of structure-specific endonucleases in response to DNA damage. *Cell Rep.* **20**, 1553–1562.

Schmekel, K. and Daneholt, B. 1995. The central region of the synaptonemal complex revealed in three dimensions. *Trends Cell Biol.* **5**, 239–242.

Song, M., Zhai, B., Yang, X., Tan, T., Wang, Y., Yang, X., Tan, Y., Chu, T., Cao, Y., Song, Y., et al. 2021. Interplay between Pds5 and Rec8 in regulating chromosome axis length and crossover frequency. *Sci. Adv.* **7**, eabe7920.

Sung, P. 1997. Function of yeast Rad52 protein as a mediator between replication protein A and the Rad51 recombinase. *J. Biol. Chem.* **272**, 28194–28197.

Sutani, T., Kawaguchi, T., Kanno, R., Itoh, T., and Shirahige, K. 2009. Budding yeast Wpl1(Rad61)-Pds5 complex counteracts sister chromatid cohesion-establishing reaction. *Curr. Biol.* **19**, 492–497.

Sym, M., Engebrecht, J.A., and Roeder, G.S. 1993. ZIP1 is a synaptonemal complex protein required for meiotic chromosome synapsis. *Cell* **72**, 365–378.

Tsubouchi, T., Macqueen, A.J., and Roeder, G.S. 2008. Initiation of meiotic chromosome synapsis at centromeres in budding yeast. *Genes Dev.* **22**, 3217–3226.

Unal, E., Heidinger-Pauli, J.M., Kim, W., Guacci, V., Onn, I., Gygi, S.P., and Koshland, D.E. 2008. A molecular determinant for the establishment of sister chromatid cohesion. *Science* **321**, 566–569.

van Heemst, D., James, F., Pöggeler, S., Berteaux-Lecellier, V., and Zickler, D. 1999. Spo76p is a conserved chromosome morphogenesis protein that links the mitotic and meiotic programs. *Cell* **98**, 261–271.

Wan, L., de los Santos, T., Zhang, C., Shokat, K., and Hollingsworth, N.M. 2004. Mek1 kinase activity functions downstream of *RED1* in the regulation of meiotic double strand break repair in budding yeast. *Mol. Biol. Cell* **15**, 11–23.

Wild, P., Susperregui, A., Piazza, I., Dörig, C., Oke, A., Arter, M., Yamaguchi, M., Hilditch, A.T., Vuina, K., Chan, K.C., et al. 2019. Network rewiring of homologous recombination enzymes during mitotic proliferation and meiosis. *Mol. Cell* **75**, 859–874.

Yoon, S.W., Lee, M.S., Xaver, M., Zhang, L., Hong, S.G., Kong, Y.J., Cho, H.R., Kleckner, N., and Kim, K.P. 2016. Meiotic prophase roles of Rec8 in crossover recombination and chromosome structure. *Nucleic Acids Res.* **44**, 9296–9314.

Zakharyevich, K., Ma, Y., Tang, S., Hwang, P.Y., Boiteux, S., and Hunter, N. 2010. Temporally and biochemically distinct activities of Exo1 during meiosis: double-strand-break resection and resolution of double-Holliday junctions. *Mol. Cell* **40**, 1001–1015.

Zhang, Z., Ren, Q., Yang, H., Conrad, M.N., Guacci, V., Kateneva, A., and Dresser, M.E. 2005. Budding yeast PDS5 plays an important role in meiosis and is required for sister chromatid cohesion. *Mol. Microbiol.* **56**, 670–680.

Zhang, J., Shi, X., Li, Y., Kim, B.J., Jia, J., Huang, Z., Yang, T., Fu, X., Jung, S.Y., Wang, Y., et al. 2008. Acetylation of Smc3 by Eco1 is required for S phase sister chromatid cohesion in both human and yeast. *Mol. Cell* **31**, 143–151.

Zhu, Z., Chung, W.H., Shim, E.Y., Lee, S.E., and Ira, G. 2008. Sgs1 helicase and two nucleases Dna2 and Exo1 resect DNA double-trand break ends. *Cell* **134**, 981–994.

Zickler, D. and Kleckner, N. 1999. Meiotic chromosomes: integrating structure and function. *Annu. Rev. Genet.* **33**, 603–754.